# Benchmark Study of DFT Functionals for Late-Transition-Metal Reactions†

**Miriam M. Quintal,‡ Amir Karton, Mark A. Iron,§ A. Daniel Boese,|| and Jan M. L. Martin***

*Department of Organic Chemistry, Weizmann Institute of Science, 76100 Rehovot, Israel*

*Received: August 9, 2005; In Final Form: September 23, 2005*

The performance of a wide variety of DFT exchange-correlation functionals for a number of late-transition-metal reaction profiles has been considered. Benchmark ab-initio reference data for the prototype reactions Pd + $H_2$, Pd + $CH_4$, Pd + $C_2H_6$ (both C−C and C−H activation), and Pd + $CH_3Cl$ are presented, while ab-initio data of lesser quality were obtained for the catalytic hydrogenation of acetone and for the low-oxidation-state and high-oxidation-state mechanisms of the Heck reaction. "Kinetics" functionals such as mPW1K, PWB6K, BB1K, and BMK clearly perform more poorly for late-transition-metal reactions than for main-group reactions, as well as compared to general-purpose functionals. There is no single "best functional" for late-transition-metal reactions, but rather a cluster of several functionals (PBE0, B1B95, PW6B95, and TPSS25B95) that perform about equally well; if main-group thermochemical performance is additionally considered, then B1B95 and PW6B95 emerge as the best performers. TPSS25B95 and TPSS33B95 offer attractive performance compromises if weak interactions and main-group barrier heights, respectively, are also important. In the ab-initio calculations, basis set superposition errors (BSSE) can be greatly reduced by ensuring that the metal spd shell has sufficient radial flexibility in the high-exponent range. Optimal HF percentages in hybrid functionals depend on the class of systems considered, increasing from anions to neutrals to cations to main-group barrier heights; transition-metal barrier heights represent an intermediate situation. The use of meta-GGA correlation functionals appears to be quite beneficial.

## 1. Introduction

Density functional theory (DFT) has become an increasingly popular tool for computational mechanistic chemistry. It combines reasonable accuracy with applicability to "real-life" systems of dozens of atoms rather than small model systems.

This is perhaps even more the case for organometallic problems, where the challenges facing routine ab-initio treatment are quite daunting, as illustrated by a recent paper[1] by de Jong et al. on the Pd + $CH_4$ reaction. (This is unlike the situation for main-group systems, where ab-initio approaches can reach sub-kcal/mol accuracy for small problems on a nearly "black box" basis.[2,3]) Our own work in the area of catalysis by late-transition-metal complexes[4−7] has likewise heavily relied on DFT.

Almost universally, the justification for doing so is either pragmatic (science as "art of the possible") or based on anecdotal evidence (qualitative or semiquantitative agreement with experiment for specific problems) rather than on rigorous benchmarking. The obstacles facing the latter are twofold: (1) the systems under study are generally too large to be subjected to a high-quality ab-initio treatment; (2) observed reaction rates cannot always be trivially translated into classical barrier heights, particularly not for reactions involving hydrogen transfer (as was amply demonstrated, inter alia, by the group of Prof. Truhlar[8] who is being honored with this issue).

There has been rather more of a benchmarking effort for small main-group reactions, for example, by the groups of Truhlar,[9,10] Handy,[11] and ourselves.[12] It was found fairly early[13,14] that GGA (generalized gradient approximation) functionals tend to severely underestimate reaction barrier heights (especially, but by no means solely, of radical hydrogen transfers), and indeed they may erroneously predict such reactions to be barrierless. The problem is mitigated for hybrid GGA functionals (such as the extremely popular B3LYP[15]), but it is still present. Following the observation by Durant[14] that BHLYP[16] (Becke half-and-half LYP, with 50% exact exchange) was much less prone to this problem than its generally more accurate sibling B3LYP (with a more typical 20% exact exchange), it has been shown repeatedly[9,17] that barrier heights can be drastically improved by increasing "exact" exchange into the 40−50% region—at the expense of seriously degraded performance for all other properties. (We note in passing that HF level calculations usually overestimate barriers, as a single determinant is generally a much better approximation for the reactants and products than for the transition state.) Perhaps the most commonly used such specialized "kinetics" functional has been mPW1K of Truhlar and coworkers.[9]

A situation in which one has to choose between one functional known to be accurate for equilibrium thermochemistry and another known to be accurate for barrier heights can be rather frustrating if one is considering several closely competing reaction pathways (see ref 7 for an example).

Very recently, two of us developed a new hybrid meta-GGA functional known as BMK (Boese−Martin for Kinetics[12]). The combination of (a) inclusion of the kinetic energy density in that functional, (b) the choice of a very flexible functional form, and (c) extensive optimization against large and diverse benchmark data sets led to a functional that is competitive with

† Part of the special issue "Donald G. Truhlar Festschrift".

* Corresponding author. E-mail: comartin@wicc.weizmann.ac.il.

‡ Present address: Department of Chemistry and Chemical Biology, Harvard University, 12 Oxford Street, Cambridge, MA 02138.

§ Present address: Department of Chemistry, University of Minnesota, Minneapolis, MN 55455-0431.

|| Present address: Institut für Nanotechnologie, Forschungszentrum Karlsruhe, Postfach 3640, 76021 Karlsruhe, Germany.

10.1021/jp054449w CCC: $33.50 
Published on Web 10/29/2005

(or superior to) B3LYP and other hybrid functionals for equilibrium properties, yet performs comparably to mPW1K[9] or other "kinetics" functionals for barrier heights.

We do note that, except for a few ligation energies of transition-metal complexes such as ferrocene, all the parametrization data used for BMK were for first- and second-row compounds and reactions thereof. For reactions in particular, the parametrization data were heavily weighted toward radical hydrogen transfers and some $S_N2$ reactions—which begs the question as to how relevant such parametrization data are to transition-metal reactions.

The purpose of the present work is to provide ab-initio reference data for some representative late-transition-metal reactions and to assess the performance of modern DFT functionals for them.

## 2. Selection of Benchmark Problems

Diefenbach et al.[18] recently published a relativistic DFT study on a number of prototype oxidative addition reactions involving bare Pd atoms: $Pd + C_2H_6 \rightarrow HPdC_2H_5$, $Pd + C_2H_6 \rightarrow (CH_3)_2$-Pd, $Pd + H_2 \rightarrow PdH_2$, and $Pd + CH_3Cl \rightarrow CH_3PdCl$. On one hand, these are the smallest possible prototype systems for a number of key activation steps (C−C, C−H, H−H, C−halide) in late-transition-metal chemistry; on the other hand, the systems are small enough that with modern computer technology very accurate ab-initio calculations are possible. We have selected these four reactions, plus $Pd + CH_4$ from de Jong et al.[1]

In addition to small prototype reactions, we wished to include some more complex systems, more representative of typical practical problems but, unfortunately, less amenable to high-accuracy ab-initio work. Our second choice was, therefore, the mechanism of the Heck reaction[19,20] as previously studied by our group. This is not only an important reaction in organic synthesis (and also is vital to several industrial and pharmaceutical processes), but also includes many important primary reactions of transition metals, such as oxidative addition (and its microscopic reverse, reductive elimination), $\beta$-hydride elimination, and ligand association/dissociation. In addition, competing $Pd^0-Pd^{II}$ and $Pd^{II}-Pd^{IV}$ pathways could provide some insight into how performance is affected by low versus high oxidation state of the central metal.

As our third choice, we selected the catalytic reduction of acetone.[21] The multiple competing pathways of this reaction were likewise the subject of a previous study in our group,[7] which included coupled cluster ab-initio calculations for model systems.

Fourth, we considered some additional problems, notably competitive C−C and C−H activation by pincer complexes, and a recently proposed "ring-walking" mechanism, using a secondary standard (see below).

Finally, we assessed performance for main-group systems using the very large and diverse benchmark data set used for the parametrization of BMK.

## 3. Computational Methods

All density functional calculations were carried out using a locally modified version of Gaussian 03, rev. C.01[22] running on the Linux farm of the Martin group. All coupled cluster ab-initio calculations were carried out using MOLPRO 2002.6[23] running on the same hardware. Some of the machines (dual Xeons) were custom-built (by Access Technologies of Rehovot, Israel) for heavy I/O, with Ultra320 SCSI RAID-0 controllers driving four 72-GB disks. On one machine (4-CPU AMD Opteron 846), two such arrays were aggregated in software using the "md" facility of Linux: for "chunk sizes" of 512 KB and up, sustained bandwidths over 300 MB/s could be achieved for both reading and writing. This machine proved essential for some of the larger coupled cluster calculations reported in this paper.

The following DFT GGA (generalized gradient approximation) and hybrid GGA exchange-correlation functionals were considered:

- B97-1, which is the reparametrization by Handy et al.[11] of Becke's B97 GGA power series-based functional[24] (21% HF exchange);
- B97-2, that is, Wilson, Bradley, and Tozer's modification[25] of B97 (likewise 21% exchange);
- PBE, Perdew, Burke, and Ernzerhof's[26] nonempirical GGA functional and its hybrid variant PBE0 (25% HF exchange, also known as PBE1PBE);
- mPW1K (modified Perdew−Wang 1-parameter for kinetics): Truhlar's modification[9] of Adamo and Barone's mPW1-PW91[27] with 42.8% Hartree−Fock exchange, includes modified Perdew−Wang exchange and Perdew and Wang's 1991 correlation functionals;[28,29]
- BLYP, that is, Becke's 1988 GGA functional[30] with Lee, Yang, and Parr's correlation functional,[31] as well as the exceedingly popular B3LYP hybrid;[32]
- BP86, Becke's 1988 exchange functional with Perdew's 1986 correlation functional;[33]
- HCTH/407, which is Boese and Handy's final parametrization[34] of the HCTH (Hamprecht−Cohen−Tozer−Handy[11]) GGA power series functional;
- Kang and Musgrave's KMLYP,[17] which combines LDA exchange and a high percentage (55.7%) of HF exchange with the LYP correlation functional;
- the B97-K (Becke 97 for kinetics) functional (42% HF exchange), obtained as a byproduct of BMK.[12]

The following meta-GGA and hybrid meta-GGA functionals were considered:

- B1B95, which combines Becke GGA exchange, 28% Hartree−Fock exchange, and the Becke95 meta-GGA correlation functional.[35] In addition, we considered varying the percentage of Hartree−Fock exchange, which is denoted B*x*B95 for *x*% HF exchange. B42B95 is equivalent to the BB1K "kinetics" functional of Truhlar.[36] That group's patch[37] to the routine bb95.F routine, circumventing numerical "0/0" errors, was applied to our local version of Gaussian 03;
- The TPSS (Tao−Perdew−Staroverov−Scuseria[38]) nonempirical functional (meta-GGA exchange, GGA correlation) and its hybrid variant TPSSh (10% HF exchange). We also considered the TPSS*x* series, with various values of the HF exchange percentage *x*;
- The TPSS*x*KCIS series, where the KCIS (Kriger−Chen−Iafrate−Savin[39]) meta-GGA correlation functional was employed instead of the TPSS correlation functional. Truhlar's TPSS1KCIS functional[40] represents $x = 13$;
- the mPW*x*B95 series, a combination of modified Perdew−Wang exchange with B95 correlation. For $x = 31$ and $x = 44$, one obtains the mPW1B95 and mPB1K functionals, respectively, of Zhao and Truhlar;[41]
- Truhlar's very recent PW6B95 and PWB6K functionals, which are empirical (6-parameter) adjustments of the mPW*x*B95 form for main-group thermochemistry and thermochemical kinetics, respectively;[42]
- Boese and Handy's $\tau$-HCTH and $\tau$-HCTH hybrid functionals;[43]

• the VSXC (Van Voorhis−Scuseria) empirical hybrid GGA functional;[44]

• Boese and Martin's BMK (Boese−Martin for kinetics[12]) reparametrization of $\tau$-HCTH hybrid.

For the benchmark ab-initio calculations on the Pd prototype reactions, the following two basis sets were used. The first, denoted "AVTZ", is a combination of the aug-cc-pVTZ basis set on the main-group elements with the Stuttgart−Dresden basis set/RECP combination[45] on Pd. On Pd, the basis set was completely decontracted and 2f1g polarization functions taken from ref 46 were added as well as a single set of diffuse functions. The spd exponents were determined by the "completeness profiles" approach of Chong,[47] while the f and g diffuse functions were obtained by minimizing the CISD energy of the atomic anion in its ground state. The additional exponents are given in Table S1 of Supporting Information.

de Jong et al.[1] reported very large basis set errors using the popular LANL2DZ basis set−RECP combination, augmented in various ways. We found (see Table S2 in Supporting Information) that the SDD and SDD+2f1g basis set−RECP combinations exhibit the same problem, albeit to a lesser extent. The addition of diffuse functions brings some succor when Pd(4s,4p) correlation is excluded, but not really when the latter is included. However, we found that BSSE could be drastically reduced—from 4.8 to 1.1 kcal/mol at the CCSD(T) level on Pd•••$CH_4$—by decontracting the spd orbitals (just decontracting the d orbitals yields a BSSE of 2.1 kcal/mol). We attribute this primarily to the need for high-exponent d functions to accommodate radial correlation from the 4d orbitals, and secondarily to the need to accommodate radial and angular (4s4p) correlation (if these subvalence orbitals are correlated).

The second basis set, denoted "AVQZ", was derived from Hirao's relativistic basis set[48] in the following manner:

(i) it was superimposed on the above-mentioned Stuttgart−Dresden RECP;

(ii) all primitives that contributed less than $10^{-3}$ to any orbital (multiplied by its degeneracy) of the ground-state Pd atom were deleted;

(iii) the resulting basis set was contracted at the Hartree−Fock level for the Pd atomic ground state, subjected to a Davidson reduction[49] and the outermost five primitives of every symmetry decontracted;

(iv) 5f4g3h basis functions were optimized at the CISD level for valence correlation in the atom;

(v) 2s1p1d diffuse functions were added by means of the aforementioned Chong basis set incompleteness profiles method.

The AVQZ basis set for Pd is given in MOLPRO inline format in Table S3 of Supporting Information.

Best estimates from these results were obtained by A+B/$L^{\alpha}$ extrapolations of the SCF (with $\alpha = 5$) and correlation (with $\alpha = 3.22$) energies, analogously to W1 theory.[50]

The basis set used for the DFT calculations on these systems, denoted apc2 henceforth, consists of the AVTZ set described above on the metal, in conjunction with Jensen's aug-pc2 basis set[51] on the remaining elements. The latter is of the same size as aug-cc-pVTZ, but was optimized for HF and DFT calculations rather than for correlated wave function ab-initio calculations.

For the remaining transition-metal systems, the SDB-aug-cc-pVDZ basis set as used elsewhere[52] was employed. This basis set combines the Dunning aug-cc-pVDZ basis set[53−55] on the main-group elements and the Stuttgart−Dresden basis set−RECP combination on the transition metals with an added f-type polarization exponent taken as the geometric average of the two f-exponents given in ref 56. In addition, s, p, d, and f diffuse functions were added to the rhodium center (0.00482, 0.00838, 0.0199, and 0.302, respectively).[56]

The BMK main-group benchmark data set is documented in great detail in ref 12, as is the near-DFT limit basis set employed in assessing the various functionals for it.

Reference geometries used were B3LYP/apc2 for the Pd model reactions, BMK/SDD for the other TM reactions, and taken from Supporting Information of ref 12 for the BMK set.

**TABLE 1: Best Ab-Initio Data (kcal/mol) for the Pd Model Reactions[a,b]**

| | Pd + $H_2$ | Pd + $C_2H_6$ | | Pd + $CH_3Cl$ | | Pd + $CH_4$ |
|---|---|---|---|---|---|---|
| | | CH ins. | CC ins. | OxAdd | $S_N2$ | CH ins. |
| Valence Correlation Only | | | | | | |
| $D_e$(complex) | 19.01 | 8.52 | 8.49 | 12.79 | 6.68 | 8.20 |
| $\Delta E^{\ddagger}_{forward}$ | 6.02 | 15.33 | 28.24 | 14.41 | 49.61 | 14.94 |
| $\Delta E^{\ddagger}_{backward}$ | −0.36 | 4.01 | 20.12 | 28.89 | 70.26 | 3.22 |
| reaction energy | 6.38 | 11.32 | 8.12 | −14.48 | −20.65 | 11.73 |
| Including Pd(4s,4p) Inner Valence Correlation | | | | | | |
| $D_e$(complex) | 20.68 | 9.57 | 9.54 | 14.17 | 7.58 | 9.26 |
| $\Delta E^{\ddagger}_{forward}$ | 5.02 | 13.84 | 27.17 | 14.25 | 49.18 | 13.51 |
| $\Delta E^{\ddagger}_{backward}$ | −0.12 | 5.05 | 21.83 | 30.64 | 72.26 | 4.22 |
| reaction energy | 5.15 | 8.80 | 5.34 | −16.39 | −23.08 | 9.29 |

[a] Pd + $H_2$ at CCSD(T)/cc-pVTZ geometry, rest at B3LYP/aug-pc2 geometry. [b] For Pd + $H_2$ at the CCSD(T)/cc-pVTZ level, the forward and reverse barriers (fully optimized) are 4.28 and 0.08 kcal/mol, respectively, with the Pd(4s,4p) subvalence electrons correlated. (At this geometry, 5.73 and −0.23 kcal/mol, respectively, with only valence electrons correlated.).

## 4. Results and Discussion

**4.1. Benchmark Ab-Initio Data for Prototype Pd Oxidative Additions.** Our best ab-initio calculations for the Pd model reactions are given in Table 1; results for the individual basis sets can be found in Table S4 of Supporting Information. As full CCSD(T) transition state optimizations proved unfeasible in all cases except one (Pd + $H_2$), we have arbitrarily used B3LYP/apc2 reference geometries.

We note that our intent is not to provide the best possible approximations to Nature, but the best results within the same framework (particularly, using the same RECP) as employed for the DFT calculations—in order to make sure we are "comparing apples with apples". For this reason, no attempts at explicit relativistic calculations were made.

The ab-initio results for the $S_N2$ reaction of Pd with $CH_3Cl$ are given in Table 1 for the sake of completeness, but these values are clearly far outside the energetic realm for typical thermochemical kinetics applications, and we have not considered them further in this work.

For one of the reactions (the Pd $H_2$ insertion), the reverse barrier is so shallow that a negative barrier height is obtained unless all geometries are fully optimized at the level of theory being considered.

In the case of Pd•••$CH_4$, we were able to estimate basis set superposition errors (see Table S2) using the counterpoise method.[57] With the AVTZ basis set, the total BSSE is 0.79 kcal/mol, of which 0.47 kcal/mol is due to $CH_4$ and 0.32 kcal/mol to the metal; with the AVQZ basis set, these values drop to 0.36, 0.12, and 0.24 kcal/mol, respectively. If (4s,4p) correlation is introduced, the Pd BSSEs increase to 0.62 and 0.36 kcal/mol, respectively. Extrapolation to the infinite-basis limit suggests residual BSSE of 0.1 kcal/mol or less with only valence correlation, and 0.2 kcal/ mol or less including (4s,4p) metal

subvalence correlation. We have, therefore, not carried out counterpoise calculations for any of the remaining systems.

In addition, we note for the Pd + $CH_4$ case (which is quite representative of the others in this regard) that the barriers are rather sensitive to the level of electron correlation. In particular, MP2 is woefully inadequate, and CCSD overestimates the forward barrier by 3−4 kcal/mol (depending on whether (4s,4p) correlation is included). We must therefore conclude that CCSD(T) is the minimum acceptable level of theory.

Furthermore, (4s,4p) subvalence correlation is found to have chemically significant effects. In general, complexation energies increase by 1 kcal/mol or more, and overall reaction energies become more exothermic by 2−3 kcal/mol. These contributions clearly cannot be neglected with impunity.

We believe our final results are accurate to about 1 kcal/mol within the Hamiltonian framework used. For Pd + $CH_4$ and the C−C insertion in Pd + $C_2H_6$, we may compare our results with the best calculated values of de Jong et al.[1,58] We find good to very good agreement; any discrepancies could be due to three sources: (a) our use of the B3LYP hybrid GGA functional, versus theirs of the BLYP pure GGA, for the reference geometries; (b) our use of RECPs versus their all-electron relativistic calculations; (c) the more extended basis sets and infinite-basis set limit extrapolations in our calculations. The smaller of our two basis sets, AVTZ, is somewhat more extensive in terms of both diffuse and angular correlation coverage than their largest set, B6, and has half its BSSE (cf. Table S2).

**4.2. Performance of DFT Functionals for Prototype Pd Oxidative Additions.** The relevant data can be found in Table 2. Let us first consider the overall RMS error. For starters, all the kinetics functionals considered (mPW1K, BB1K, PWB6K, and BMK) perform much more poorly than the others. The failure of BMK—broadly accurate for both main-group thermochemistry and main-group thermochemical kinetics—is particularly dramatic.

Detailed consideration of the BMK results reveals that while the forward barriers are predicted quite well, the reverse barriers (and hence reaction energies) are grossly overestimated. As all these reactions involve formally raising the oxidation state of the metal from $Pd^0$ to $Pd^{II}$, this may not be unrelated to the fact that BMK, uniquely among these functionals, underestimates the first two ionization potentials of a Pd atom by about 1 eV (see Supporting Information, Table S5). This effect is expected to be mitigated in complexes versus the bare metal, and we do find that BMK errors for the other systems are much smaller (see below).

At the other extreme from BMK is the surprisingly good performance of PBE0 (root-mean-square deviation, RMSD = 0.8 kcal/mol), approached only by two "nonstandard" mPW*x*B95 hybrids, mPW25B95 and mPW28B95 (RMSD = 0.9 kcal/mol in both cases). TPSS25B95 clocks in at 1.2 kcal/mol. Other functionals take a middle position, ranging from B1B95 (RMSD = 1.35 kcal/mol) to B3LYP (RMSD = 2.2 kcal/mol).

Inspection of the individual errors reveals that many of the functionals have substantially larger errors for the entry-channel complexation energies than for the forward and reverse barriers (and the reaction energies). If we consider the RMSD without complexation energies, the "kinetics functionals"/"general purpose functionals" dichotomy remains, but finer distinctions appear among the latter group. Most notably, the best performer now becomes B1B95 (RMSD = 0.6 kcal/ mol), no longer handicapped by its notoriously poor performance for weak interactions. PBE0 and the nonstandard hybrid mPW28B95 both

**TABLE 2: Errors in kcal/mol for Various Functionals Relative to the CCSD(T) Data in Table 1**

| | | B3LYP | B97-1 | PBE0 | B1B95 | TPSS25 TPSS | TPSS21 KCIS | TPSS25 KCIS | TPSS25 B95 | MPW B95 | mPW28 B95 | mPW25 B95 | PW6 B95 | mPW1K | BB1K | PWB6K | BMK |
|---|---|---|---|---|---|---|---|---|---|---|---|---|---|---|---|---|---|
| H−H | $\Delta E_{complex}$ | 1.75 | 0.71 | −1.23 | 1.77 | 1.60 | 1.95 | 2.56 | 2.78 | 1.28 | 0.73 | 0.18 | 2.01 | 3.20 | 4.08 | 4.36 | 1.40 |
| | $\Delta E^{\ddagger}_{forward}$ | −0.32 | −0.85 | −0.68 | 0.00 | 0.04 | 0.21 | 0.74 | 0.60 | 0.46 | 0.02 | −0.42 | 0.63 | 2.05 | 2.03 | 3.09 | −3.51 |
| | $\Delta E^{\ddagger}_{reverse}$ | 0.70 | 0.55 | −0.18 | −0.27 | 0.27 | 0.21 | 0.07 | 0.18 | −0.39 | −0.29 | −0.19 | −0.12 | −0.64 | −0.73 | −0.78 | 3.33 |
| | $\Delta E_{react}$ | −1.02 | −1.40 | −0.49 | 0.27 | −0.23 | 0.00 | 0.67 | 0.41 | 0.85 | 0.31 | −0.23 | 0.75 | 2.69 | 2.77 | 3.87 | −6.84 |
| ethane C−H | $\Delta E_{complex}$ | 3.74 | 2.45 | 1.16 | 2.61 | 2.58 | 3.04 | 3.52 | 1.23 | 1.75 | 1.40 | 1.04 | 2.10 | 4.30 | 3.95 | 3.42 | 1.23 |
| | $\Delta E^{\ddagger}_{forward}$ | 0.68 | −0.51 | −0.80 | 0.59 | 0.61 | 0.68 | 1.74 | 1.00 | 1.39 | 0.52 | −0.35 | 1.80 | 4.62 | 4.63 | 6.63 | −0.09 |
| | $\Delta E^{\ddagger}_{reverse}$ | 2.30 | 1.96 | 0.31 | −0.07 | 1.29 | 1.14 | 0.79 | 0.72 | −0.28 | −0.11 | 0.06 | 0.20 | −0.90 | −0.87 | −0.94 | 8.30 |
| | $\Delta E_{react}$ | −1.62 | −2.47 | −1.10 | 0.66 | −0.67 | −0.46 | 0.95 | 0.29 | 1.67 | 0.63 | −0.42 | 1.60 | 5.52 | 5.50 | 7.57 | −8.38 |
| ethane C−C | $\Delta E_{complex}$ | 3.71 | 2.42 | 1.13 | 2.58 | 2.55 | 3.01 | 3.49 | 1.20 | 1.72 | 1.37 | 1.39 | 2.07 | 4.27 | 3.92 | 3.39 | 1.20 |
| | $\Delta E^{\ddagger}_{forward}$ | 1.95 | 0.25 | 0.19 | −0.03 | 0.62 | 0.83 | 1.95 | −1.05 | 0.61 | −0.26 | −1.52 | 0.97 | 5.67 | 4.00 | 5.82 | 0.57 |
| | $\Delta E^{\ddagger}_{reverse}$ | 4.07 | 3.29 | 0.66 | −0.70 | 2.06 | 2.05 | 1.52 | 0.18 | −1.22 | −0.93 | −0.64 | −0.33 | −0.99 | −2.09 | −2.35 | 11.62 |
| | $\Delta E_{react}$ | −2.12 | −3.05 | −0.47 | 0.67 | −1.44 | −1.23 | 0.43 | −1.23 | 1.83 | 0.66 | −0.89 | 1.30 | 6.66 | 6.10 | 8.17 | −11.05 |
| $CH_3$−Cl | $\Delta E_{complex}$ | 3.05 | 1.92 | 1.08 | 3.13 | 2.28 | 2.68 | 3.36 | 1.36 | 2.51 | 2.04 | 1.55 | 2.65 | 4.82 | 5.00 | 4.67 | 1.20 |
| | $\Delta E^{\ddagger}_{forward}$ | 0.51 | −0.43 | −0.55 | −1.24 | −0.66 | −0.38 | 0.23 | −2.23 | −1.02 | −1.45 | −1.89 | −0.95 | 2.32 | 0.71 | 1.41 | 0.15 |
| | $\Delta E^{\ddagger}_{reverse}$ | 1.76 | 1.87 | −0.02 | −1.15 | 1.79 | 1.09 | 0.76 | 0.16 | −1.58 | −1.35 | −1.13 | −1.15 | −1.01 | −2.25 | −2.62 | 14.75 |
| | $\Delta E_{react}$ | −1.24 | −2.31 | −0.52 | −0.09 | −2.44 | −1.47 | −0.53 | −2.39 | 0.56 | −0.10 | −0.76 | 0.20 | 3.33 | 2.96 | 4.03 | −14.60 |
| $CH_4$ | $\Delta E_{complex}$ | 3.35 | 2.09 | 0.69 | 2.16 | 2.14 | 2.62 | 3.10 | 0.88 | 1.40 | 1.06 | 0.70 | 1.82 | 3.83 | 3.50 | 3.11 | 0.94 |
| | $\Delta E^{\ddagger}_{forward}$ | 0.27 | −0.87 | −1.07 | 0.40 | 0.19 | 0.25 | 1.26 | 0.89 | 1.16 | 0.36 | −0.44 | 1.52 | 4.08 | 4.12 | 5.96 | −0.86 |
| | $\Delta E^{\ddagger}_{reverse}$ | 2.10 | 1.81 | 0.16 | −0.17 | 1.23 | 1.03 | 0.72 | 0.83 | −0.44 | −0.23 | −0.02 | 0.13 | −0.79 | −1.15 | −1.27 | 8.07 |
| | $\Delta E_{react}$ | −1.83 | −2.68 | −1.23 | 0.58 | −1.04 | −0.78 | 0.54 | 0.06 | 1.60 | 0.59 | −0.43 | 1.39 | 4.87 | 5.27 | 7.24 | −8.92 |
| RMS error | | 2.22 | 1.92 | 0.79 | 1.35 | 1.53 | 1.58 | 1.83 | 1.32 | 1.23 | 0.90 | 0.89 | 1.40 | 3.78 | 3.66 | 4.59 | 7.25 |
| RMS error, no complexation | | 1.78 | 1.89 | 0.66 | 0.59 | 1.20 | 0.96 | 1.00 | 1.13 | 1.06 | 0.67 | 0.81 | 1.04 | 3.66 | 3.49 | 4.82 | 8.34 |

**TABLE 3: RMSD (kcal/mol) for the Heck Reaction and Hydrogenation of Acetone**

| | Pd activation reactions | | Heck reaction | | | | |
|---|---|---|---|---|---|---|---|
| | with complexation | without complexation | with complexation | without complexation | acetone | overall TM performance | main-group performance |
| B3LYP | 2.22 | 1.78 | 4.39 | 2.49 | 2.10 | 2.14 | 7.54 |
| B97-1 | 1.92 | 1.89 | 3.05 | 1.97 | 1.34 | 1.76 | 5.52 |
| PBE0 | 0.79 | 0.66 | 2.85 | 1.92 | 1.70 | 1.53 | 6.68 |
| B1B95 | 1.35 | 0.59 | 2.73 | 1.60 | 1.89 | 1.47 | 5.15 |
| TPSS25TPSS | 1.53 | 1.20 | 3.22 | 2.36 | 1.11 | 1.66 | 11.94 |
| TPSS21KCIS | 1.58 | 0.96 | 3.28 | 1.92 | 1.57 | 1.54 | 7.38 |
| TPSS25KCIS | 1.83 | 1.00 | 3.37 | 1.98 | 1.43 | 1.52 | 8.61 |
| mPW1B95 | 1.32 | 1.13 | 2.43 | 1.58 | 1.76 | 1.51 | 5.72 |
| mPW28B95 | 0.90 | 0.67 | 2.38 | 1.53 | 2.03 | 1.52 | 6.12 |
| mPW25B95 | 0.89 | 0.81 | 2.37 | 1.55 | 2.39 | 1.71 | 6.96 |
| PW6B95 | 1.40 | 1.04 | 2.47 | 1.57 | 1.68 | 1.46 | 4.81 |
| mPW1K | 3.78 | 3.66 | 3.94 | 3.10 | 2.70 | 3.18 | 14.67 |
| BB1K | 3.66 | 3.49 | 3.14 | 2.27 | 2.07 | 2.68 | 9.49 |
| PWB6K | 4.60 | 4.76 | 3.15 | 2.61 | 2.87 | 3.55 | 10.42 |
| BMK | 7.25 | 8.34 | 4.02 | 3.53 | 3.84 | 5.68 | 5.53 |
| BP86 | 6.07 | 6.72 | 3.65 | 2.97 | 5.98 | 5.47 | 21.2 |
| BLYP | 4.90 | 5.59 | 5.01 | 3.42 | 4.56 | 4.61 | 10.3 |
| PBE | 5.82 | 6.30 | 3.30 | 2.84 | 6.02 | 5.29 | 18.9 |
| VSXC | 3.77 | 2.96 | 7.34 | 6.73 | 5.15 | 5.18 | 7.8 |
| B97-2 | 2.20 | 0.76 | 4.10 | 2.32 | 1.87 | 1.78 | 5.3 |
| $\tau$-HCTH | 3.49 | 3.62 | 4.49 | 2.88 | 3.99 | 3.53 | 7.1 |
| $\tau$-HCTHh | 3.16 | 3.61 | 2.95 | 2.04 | 2.19 | 2.71 | 5.5 |
| HCTH/407 | 3.16 | 2.46 | 5.68 | 3.32 | 3.94 | 3.30 | 7.9 |
| KMLYP | 5.04 | 5.78 | 4.36 | 4.05 | 3.84 | 4.64 | 25.6 |
| B97-K | 4.30 | 3.41 | 4.26 | 3.01 | 3.77 | 3.41 | 10.3 |

come very close (0.7 kcal/mol), but TPSS21KCIS, TPSS25KCIS, TPSS25B95, and PW6B95 all hover around the 1 kcal/mol mark. Traditional thermochemistry hybrid GGAs such as B3LYP and B97-1 are seen to be noticeably poorer (1.8 and 1.9 kcal/mol, respectively).

The excellent performance of the B95 correlation functional (see also refs 41,42) is somewhat surprising, considering that this functional was disavowed by its own developer[24] because of its problems with weak interactions. However, we shall see that, given the performance of B1B95 and PW6B95 (and, to a lesser extent, TPSS25B95), reports of the demise of B95 appear to be quite premature.

In two very recent papers, de Jong et al.[58,59] compared a large number of pure GGA and meta-GGA functionals (plus the B3LYP and TPSSh hybrid functionals) to their earlier relativistic coupled cluster calculations[1,58] for Pd + $CH_4$ and the C−C insertion pathway of Pd + $C_2H_6$. Aside from the different focus, a direct comparison between their work and our work is somewhat hampered by the different reference data and reference geometries, and to a lesser extent by the different basis sets used (large Gaussian vs Slater basis sets). Insofar as a comparison is possible, our results are in good agreement.

**4.3. Other TM Reactions.** We shall now turn to the Heck reaction and to the hydrogenation of acetone. Detailed results are available as Supporting Information to this paper (Tables S6 and S7), while a summary is presented in Table 3.

As both the reference data and the DFT calculations were obtained with considerably smaller basis sets, comparisons are somewhat influenced by BSSE, and in particular complexation steps have to be eliminated to make any meaningful distinctions possible. This being said, we find the following.

BMK's failure appears to be much less dramatic in these two cases, yet it is still there. Likewise, the kinetics functionals appear to perform less well than their "general purpose" siblings, and the B95 correlation functional once again acquits itself very well. It is difficult, however, to make finer distinctions.

We further considered two additional reactions we previously studied: competitive C−C versus C−H activation by rhodium−PCP "pincer complexes,"[5] and a recently published "ring-walking" mechanism.[6] As coupled cluster calculations were out of the question here, we used PBE0 as a "secondary standard" with basis sets of SDB-cc-pVDZ (rhodium−PCP) and SDB-cc-pVTZ[46] (ring-walking) quality.

The results (see Tables S8 and S9 in Supporting Information) are basically that the B95-based functionals cluster closely to the PBE0 results, and that kinetics functionals systematically overestimate barriers, while traditional hybrid GGAs such as B3LYP and B97-1 take a middle position.

**4.4. Performance for Main-Group Systems.** We now turn to the BMK evaluation set, which contains more than 400 thermochemical properties (including 24 transition states) as well as several thousand gradient components (Tables 4 and 5). If we consider the overall RMS error, B1B95 puts in the best performance (5.06 kcal/mol), followed by B97-1 (5.32 kcal/mol), while BMK and mPW1B95 tie for third place (5.58 kcal/mol).

The overall performance of both PW6B95 and PWB6K is adversely impacted by these functionals' serious errors for atomic absolute energies. If we remove the latter from the comparison, the overall picture changes. PW6B95 is now found to have the smallest overall RMS error (4.81 kcal/mol) followed by B1B95 (5.15 kcal/ mol), a virtual tie between B97-1 and BMK (5.52 and 5.53 kcal/mol, respectively), mPW1B95 (5.72 kcal/mol), and TPSS20B95 (5.82 kcal/mol). The rather good performances by TPSSh and TPSS1KCIS (6.01 and 6.18 kcal/mol, respectively) are marred by errors for main-group transition states that meet or exceed that of B3LYP. For functionals with HF exchange percentages more suitable for late-transition-metal reactions (e.g., TPSS21KCIS or TPSS25KCIS), the performance for main-group transition states improves appreciably, but this is outweighed by serious deterioration for neutral and anionic molecules. PBE0 clocks in at 6.68 kcal/mol, again with near-B3LYP errors for main-group transition states and somewhat poor performance for neutrals and anions—but overall still better than B3LYP (7.74 kcal/mol). Of the "kinetics" functionals considered, BMK is the only one that yields a consistently good

**TABLE 4: RMS Errors (kcal/mol) of Various Functionals for the BMK Main-Group Data Set and Various Subsets Thereof**

| | gradients | reaction energies | all neutrals | cationic molecules | cations from PAs | all cations | anionic molecules | all anions | transition states | everything | everything w/o atoms |
|---|---|---|---|---|---|---|---|---|---|---|---|
| no. of systems | | 62 | 219 | 64 | 8 | 88 | 47 | 58 | 24 | 404 | |
| B3LYP | 10.41 | 4.43 | 8.14 | 5.73 | 2.69 | 5.72 | 8.11 | 9.08 | 5.04 | 7.77 | 7.74 |
| B971 | 10.01 | 4.17 | 4.77 | 6.12 | 4.15 | 5.48 | 6.90 | 6.29 | 5.20 | 5.32 | 5.52 |
| PBE0 | 12.33 | 4.29 | 8.49 | 7.72 | 4.97 | 11.78 | 6.65 | 9.70 | 4.92 | 9.32 | 6.68 |
| B1B95 | 12.18 | 3.06 | 4.34 | 6.44 | 1.69 | 5.79 | 7.16 | 6.58 | 3.54 | 5.06 | 5.15 |
| TPSSh | 10.44 | 5.50 | 7.31 | 8.40 | 6.60 | 9.51 | 8.08 | 8.40 | 6.8 | 6.22 | 6.01 |
| TPSS25TPSS | 11.68 | 4.59 | 12.65 | 11.20 | 6.26 | 10.09 | 12.99 | 11.91 | 4.79 | 11.55 | 11.94 |
| TPSS1KCIS | 11.68 | 4.44 | 6.18 | 7.79 | 3.65 | 7.78 | 7.02 | 7.63 | 5.14 | 6.65 | 6.18 |
| TPSS21KCIS | 12.21 | 3.78 | 7.64 | 7.09 | 3.40 | 7.02 | 9.14 | 8.80 | 3.99 | 7.50 | 7.38 |
| TPSS25KCIS | 13.17 | 3.60 | 9.07 | 7.26 | 3.34 | 7.03 | 10.48 | 9.78 | 3.39 | 8.53 | 8.61 |
| mPW1B95 | 13.64 | 3.04 | 5.13 | 7.39 | 2.03 | 6.56 | 6.65 | 6.13 | 3.71 | 5.58 | 5.72 |
| mPW28B95 | 12.40 | 3.05 | 5.87 | 7.92 | 2.38 | 7.02 | 5.94 | 5.53 | 4.24 | 5.97 | 6.12 |
| mPW25B95 | 11.39 | 3.13 | 7.09 | 8.66 | 2.76 | 7.65 | 5.61 | 5.28 | 4.79 | 6.76 | 6.96 |
| PW6B95 | 12.28 | 2.82 | 11.86 | 5.85 | 1.95 | 17.40 | 6.60 | 17.20 | 3.79 | 13.67 | 4.81 |
| mPW1K | 19.16 | 4.81 | 15.84 | 11.46 | 7.37 | 10.17 | 15.47 | 13.94 | 1.80 | 14.02 | 14.67 |
| BB1K | 18.87 | 3.31 | 9.60 | 7.65 | 1.71 | 6.75 | 12.42 | 11.28 | 1.75 | 9.12 | 9.49 |
| PWB6K | 21.78 | 3.73 | 12.45 | 8.80 | 3.50 | 12.65 | 12.74 | 14.03 | 1.65 | 12.39 | 10.42 |
| BMK | 12.58 | 3.69 | 4.49 | 6.97 | 2.36 | 6.60 | 8.42 | 7.86 | 1.96 | 5.58 | 5.53 |
| TPSS20B95 | 10.30 | 4.73 | 6.46 | 6.57 | 4.58 | 8.26 | 7.94 | 8.77 | 4.31 | 7.06 | 5.82 |
| TPSS25B95 | 11.89 | 4.25 | 7.22 | 6.45 | 4.66 | 7.97 | 9.47 | 9.58 | 3.52 | 7.51 | 6.66 |
| TPSS33B95 | 15.58 | 3.72 | 9.89 | 7.43 | 4.89 | 8.26 | 12.29 | 11.55 | 2.43 | 9.43 | 9.19 |
| TPSS42B95 | 20.34 | 3.63 | 13.71 | 9.59 | 5.26 | 9.49 | 15.67 | 14.27 | 1.64 | 12.44 | 12.68 |

**TABLE 5: RMS Errors for Additional Subsets of the BMK Data Set**

| | neutral molecules | non-hydrogen systems | non-hydrogen hydrocarbons | substituted hydrocarbons | radicals | inorganic hydrides | hydrogen-bonded dimers | dissociation complexes |
|---|---|---|---|---|---|---|---|---|
| no. of systems | 209 | 71 | 27 | 46 | 38 | 27 | 4 | 5 |
| B3LYP | 7.86 | 11.76 | 5.71 | 4.82 | 3.10 | 5.33 | 0.43 | 17.95 |
| B971 | 4.85 | 5.48 | 5.58 | 4.84 | 3.35 | 3.99 | 0.14 | 13.11 |
| PBE0 | 6.44 | 7.12 | 9.49 | 5.68 | 3.46 | 5.05 | 0.19 | 14.33 |
| B1B95 | 4.33 | 5.65 | 3.38 | 4.01 | 2.31 | 3.83 | 1.04 | 9.41 |
| TPSS25TPSS | 12.82 | 18.03 | 4.96 | 9.37 | 7.61 | 12.72 | 0.37 | 14.78 |
| TPSS21KCIS | 7.47 | 10.82 | 3.34 | 4.56 | 3.78 | 7.57 | 0.34 | 12.13 |
| TPSS25KCIS | 9.05 | 13.21 | 2.99 | 5.92 | 4.42 | 8.86 | 0.34 | 15.43 |
| mPW1B95 | 5.15 | 5.75 | 7.29 | 5.05 | 2.82 | 3.31 | 0.43 | 10.07 |
| mPW28B95 | 5.91 | 6.28 | 8.42 | 6.29 | 3.65 | 3.13 | 0.43 | 7.81 |
| mPW25B95 | 7.17 | 7.72 | 9.60 | 7.81 | 4.72 | 3.71 | 0.44 | 5.62 |
| PW6B95 | 3.98 | 5.20 | 3.52 | 3.34 | 2.35 | 3.57 | 0.31 | 10.42 |
| mPW1K | 16.20 | 22.24 | 7.42 | 14.58 | 8.37 | 14.68 | 0.36 | 28.32 |
| BB1K | 9.79 | 13.40 | 4.53 | 8.71 | 5.05 | 9.19 | 0.86 | 19.67 |
| PWB6K | 10.86 | 14.95 | 4.20 | 9.34 | 6.07 | 10.34 | 0.22 | 22.32 |
| BMK | 4.37 | 6.18 | 2.16 | 3.43 | 3.15 | 2.95 | 0.60 | 11.30 |

performance, with BB1K a distant second, PWB6K an even more distant third, and TPSS42B95 a still worse fourth. TPSS33B95 strikes a peculiar compromise between main-group overall RMSD (9.19 kcal/mol), RMSD for main-group transition states (2.4 kcal/mol), and ditto for the Pd reactions (2.0 kcal/mol). The best performances for main-group transition states taken in isolation are seen for PWB6K and TPSS42B95 (both RMSD = 1.6 kcal/mol), followed by the triad of BB1K, mPW1K, and TPSS42KCIS (all 1.8 kcal/mol), in turn followed by BMK (2.0 kcal/mol).

If we consider subclasses of the neutral molecules, we note that BB1K and PWB6K actually do excellent jobs for hydrocarbons, but sharply deteriorate for more "inorganic" species (the 71 non-hydrogen systems and the 27 inorganic hydrides). Their non-"kinetics" siblings, B1B95 and PW6B95, respectively, show excellent performance across all subcategories. As expected, B1B95 and BB1K are the worst performers for hydrogen bonds, whereas PW6B95 and PWB6K represent significant improvements, as does the TPSS*x*B95 series.

Some light might be shed on the above by considering the dependence of errors in the various categories as a function of the percentage of Hartree−Fock exchange. We have done so in Figure 1 for TPSS exchange combined with the KCIS correlation functional.

For neutral molecules, the optimum is at the 13% adopted by Truhlar and co-workers for their TPSS1KCIS functional. For anions, however, a smaller percentage (10%) is preferred, while for cations the optimum lies at 25%. (The optimum for gradients is very close to that for neutrals, at 14%.) For reaction energies, the minimum can be found around 30%, but the curve is very flat and all values between 20 and 42% yield roughly comparable performance. For main-group transition states, we find the minimum around 42% (the percentage of HF exchange used in BMK and BB1K), with performance deteriorating sharply as the percentage of HF exchange is reduced below 33−35%. For the Pd reactions, we find our minimum around 20%, although the curve is quite flat between 15 and 25% and appreciable degradation is only seen outside this interval. The hydrogenation of acetone and the Heck reaction both exhibit minima around 25%, but especially for the Heck reaction the response curve is very flat and any percentage between 20 and 25% is close to optimum for all three TM reaction sets.

A similar graph is obtained for the B*x*B95 series (Figure 2), but the minima for the neutrals, cations, and anions are shifted considerably to the right. The minima are at 21, 28, and 33%, respectively, and the cation response is quite flat in the 25−40% region, as is the response for the Pd reactions in the 20−35% range. 25% and 28% (aka B1B95) are actually quite good

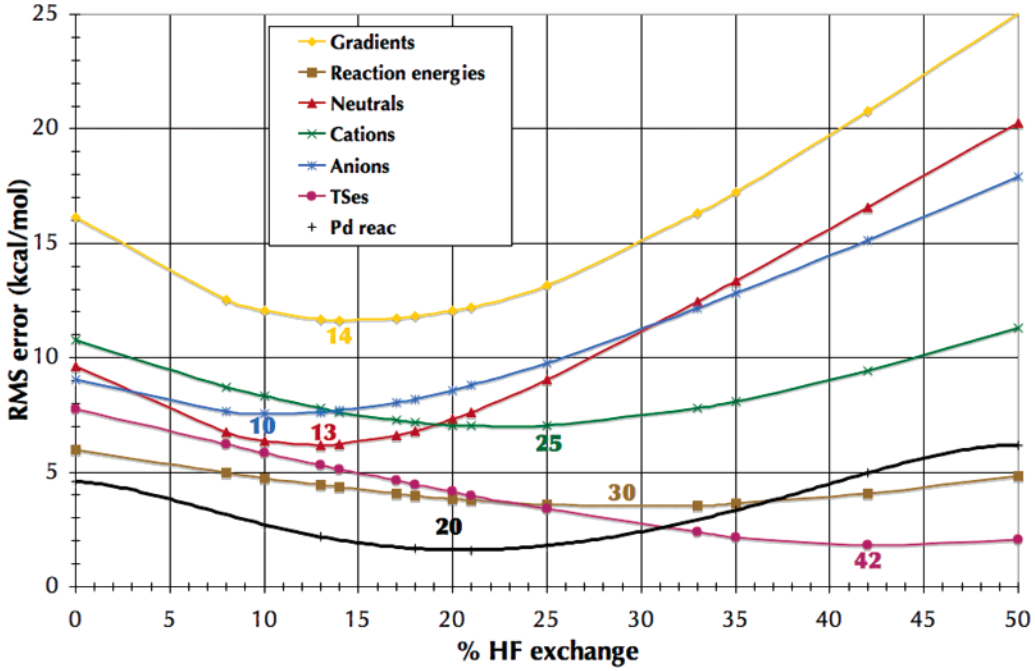


**Figure 1.** Dependence of TPSS*x*KCIS RMS errors (kcal/mol) for various types of systems as a function of the % of Hartree−Fock exchange *x*.

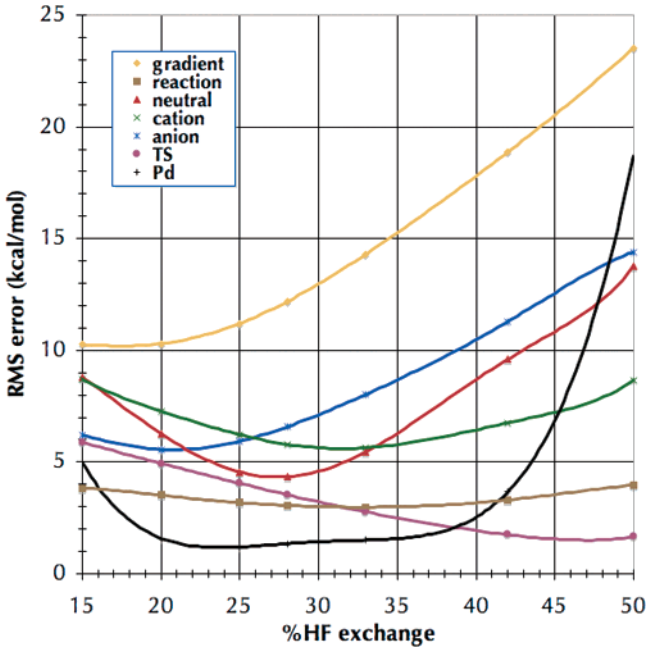


**Figure 2.** Dependence of B*x*B95 RMS errors (kcal/mol) for various types of systems as a function of the % of Hartree−Fock exchange *x*.

compromises between the various requirements (except for the main-group transition states).

Finally, gradients at the equilibrium geometry—a convenient metric for geometry performance—have an optimum of 14% for TPSS*x*KCIS (Figure 1) and about 19% for B*x*B95 (Figure 2). The response is, however, quite flat in the neighborhood of these values, between 10 and 20%, and only above 25−30% is a sharp deterioration observed. In general, we see in Tables 4 and 5 that the kinetics functionals—except for BMK—yield much worse performance for geometries than more general-purpose hybrids, which is consistent with our earlier observations for geometries and anharmonic force fields.[60]

## 5. Conclusions

From the above study, we can conclude the following:

(a) There is no one "best DFT functional" for late-transition-metal reactions, but rather a cluster of 5−6 functionals that perform about equally well: PBE0, B1B95, PW6B95, TPSS-25B95, and perhaps B97-1 and/or B97-2. Differentiation within this group is possible when performance for other properties is considered. Surprisingly, the much-maligned B1B95 functional (disavowed by its own author[24]) performs remarkably well; overall best performances are turned in by B1B95 and PW6B95, the former of which has an advantage for main-group reaction barriers and the latter for weak molecular interactions. TPSS25B95 and TPSS33B95 offer interesting performance compromises, the latter favoring main-group transition states more than the former.

(b) To reduce BSSE in the ab-initio calculations, it is essential to use basis sets on the metal with sufficient radial flexibility, especially in the d orbitals. Subvalence correlation on the metal is chemically significant, and its correct treatment requires adequate high-exponent d functions: the best way to realize this appears to be to decontract the 3d orbital in the basis set.

(c) For hybrid GGA (and meta-GGA) functionals, the optimal percentage of Hartree−Fock-type exchange depends on the property considered.

a. For molecular binding energies, the optimal percentage increases from anions to neutral species to cations.

b. Main-group barrier heights require the largest amounts of exact exchange, while transition-metal reactions appear to take an intermediate position.

(d) "Kinetics" functionals such as mPW1K and BMK—successful as they are for main-group thermochemical kinetics—do not fare well for late-transition-metal barrier heights.

(e) BMK exhibits a particular weakness for reactions involving metals in low oxidation states (e.g., $Pd^{0}-Pd^{II}$).

(f) The use of meta-GGA correlation functionals appears to be quite beneficial: witness not only the performance of B1B95 and PW6B95, but also the consistently better performance of hybrid TPSSKCIS relative to hybrid TPSS. The improvement

is much more pronounced than for meta-GGA exchange, where $\tau$-HCTH hybrid only represents a marginal improvement over its hybrid GGA counterpart B97-1. This issue requires further investigation.

Work is presently in progress on the development of a successor to BMK that performs better for late-transition-metal reactions.

**Acknowledgment.** This work was supported by the Israel Science Foundation (Grant 704/05), by the Lise Meitner-Minerva Center for Computational Quantum Chemistry, and by the Helen and Martin Kimmel Center for Molecular Design. M.M.Q. acknowledges a Fulbright fellowship from the United States−Israel Educational Foundation. J.M.L.M. is the Baroness Thatcher Professor of Chemistry.

**Supporting Information Available:** Full refs 22 and 23; Additional Pd AVTZ basis set exponents (Table S1); BSSE as a function of the basis set for the Pd···$CH_4$ complex (Table S2); Pd AVQZ basis set (Table S3); CCSD(T)/AVTZ and CCSD-(T)/AVQZ results for the Pd model reactions (Table S4); ionization potentials of Pd (Table S5). Tables S6−S9 contain overall energetics for the following reactions: Heck, catalytic hydrogenation of acetone by Rh(I), CC and CH activation by Rh(I), and ring-walking.

## References and Notes

(1) de Jong, G. T.; Solà, M.; Visscher, L.; Bickelhaupt, F. M. *J. Chem. Phys.* **2004**, *121*, 9982.

(2) Martin, J. M. L.; de Oliveira, G. *J. Chem. Phys.* **1999**, *111*, 1843; Parthiban, S.; Martin, J. M. L. *J. Chem. Phys.* **2001**, *114*, 6014; Martin, J. M. L.; Parthiban, S. In *Quantum Mechanical Prediction of Thermochemical Data*; Cioslowski, J., Ed.; (Understanding Chemical Reactivity series, Vol. 22), Kluwer Academic Publishers: Dordrecht (The Netherlands), August 2001; Chapter 2, pp 31−65; Boese, A. D.; Oren, M.; Atasoylu, O.; Martin, J. M. L.; Kállay, M.; Gauss, J. *J. Chem. Phys.* **2004**, *120*, 4129.

(3) Tajti, A.; Szalay, P. G.; Császár, A. G.; Kállay, M.; Gauss, J.; Valeev, E. F.; Flowers, B. A.; Vasquez, J.; Stanton, J. F. *J. Chem. Phys.* **2004**, *121*, 11599.

(4) Sundermann, A.; Uzan, O.; Martin, J. M. L. *Chem. Eur. J.* **2001**, *7*, 1703.

(5) Sundermann, A.; Uzan, O.; Milstein, D.; Martin, J. M. L. *J. Am. Chem. Soc.* **2000**, *122*, 7095.

(6) Strawser, D.; Karton, A.; Iron, M. A.; Zenkina, O.; Martin, J. M. L.; van der Boom, M. E. *J. Am. Chem. Soc.* **2000**, *122*, 7095.

(7) Iron, M. A.; Sundermann, A.; Martin, J. M. L. *J. Am. Chem. Soc.* **2003**, *125*, 11430.

(8) Garrett, B. C.; Truhlar, D. G. In *Physical and Chemical Aspects of Hydrogen Transfer*; Hynes, J. T., Limbach, H. H., Eds.; Handbook of Hydrogen Transfer, Vol. 1; edited by Schowen, R. L., Ed.; Wiley-VCH: Weinheim, Germany, 2005.

(9) Lynch, B. J.; Fast, P. L.; Harris, M.; Truhlar, D. G. *J. Phys. Chem. A* **2000**, *104*, 4811.

(10) Zhao, Y.; Lynch, B. J.; Truhlar, D. G. *J. Phys. Chem. A* **2004**, *108*, 2715.

(11) Hamprecht, F. A.; Cohen, A. J.; Tozer, D. J.; Handy, N. C. *J. Chem. Phys.* **1998**, *109*, 6264−6271.

(12) Boese, A. D.; Martin, J. M. L. *J. Chem. Phys.* **2004,** *121*, 3405.

(13) Baker, J.; Andzelm, J.; Muir, M.; Taylor, P. R. *Chem. Phys. Lett.* **1995**, *232*, 53.

(14) Durant, J. L. *Chem. Phys. Lett.* **1996**, *256*, 595.

(15) Becke, A. D. *J. Chem. Phys.* **1993**, *98*, 5648.

(16) Becke, A. D. *J. Chem. Phys.* **1993**, *98*, 1372.

(17) Kang, J. K.; Musgrave, C. B. *J. Chem. Phys.* **2001**, *115*, 11040.

(18) Diefenbach, A.; de Jong, G. T.; Bickelhaupt, F. M. *J. Chem. Theory Comput.* **2005**, *1*, 286.

(19) Mizoroki, T.; Mori, K.; Ozaki, A. *Bull. Chem. Soc. Jpn.* **1971**, *44*, 581.

(20) Heck, R. F.; Nolley, J. P., Jr. *J. Org. Chem.* **1972**, *37*, 2320.

(21) Töllner, K.; Popovitz-Biro, R.; Lahav, M.; Milstein, D. *Science* **1997**, *278*, 2100.

(22) Frisch, M. J., et al. *Gaussian 03*, revision C.01; Gaussian, Inc.: Pittsburgh, PA, 2003; see Supporting Information for full reference.

(23) MOLPRO is a package of ab-initio programs written by Werner, H.-J., Knowles, P. J. et al.; http://www.molpro.net; see Supporting Information for full reference.

(24) Becke, A. D. *J. Chem. Phys.* **1997**, *107*, 8554.

(25) Wilson, P. J.; Bradley, T. J.; Tozer, D. J. *J. Chem. Phys.* **2001**, *115*, 9233.

(26) Perdew, J. P.; Burke, K.; Ernzerhof, M. *Phys. Rev. Lett.* **1996**, *77*, 3865.

(27) Adamo, C.; Barone, V. *J. Chem. Phys.* **1998**, *108*, 664.

(28) Perdew, J. P. In *Electronic Structure of Solids*; Ziesche, P., Eschig, H., Eds.; Akademie Verlag: Berlin, 1991; p 11.

(29) Burke, K.; Perdew, J. P.; Wang, Y. In *Electronic Density Functional Theory: Recent Progress and New Directions*; Dobson, J. F., Vignale, G., Das, M. P., Eds.; Plenum: New York, 1998; p 81.

(30) Becke, A. D. *Phys. Rev. A* **1988**, *38*, 3098.

(31) Lee, C.; Yang, W.; Parr, R. G. *Phys. Rev. B* **1988**, *37*, 785.

(32) Stevens, P. J.; Devlin, F. J.; Chabalowski, C. F.; Frisch, M. J. *J. Phys. Chem.* **1994**, *98*, 11623.

(33) Perdew, J. P. *Phys. Rev. B* **1986**, *33*, 8822.

(34) Boese, A. D.; Handy, N. C. *J. Chem. Phys.* **2001**, *114*, 5497.

(35) Becke, A. D. *J. Chem. Phys.* **1996**, *104*, 1040.

(36) Zhao, Y.; Lynch, B. J.; Truhlar, D. G. *J. Phys. Chem. A* **2004**, *108*, 2715.

(37) Zhao, Y.; Truhlar, D. G. *J. Chem. Theory Comput.* **2005**, *1*, 415.

(38) Tao, J. M.; Perdew, J. P.; Staroverov, V. N.; Scuseria, G. E. *Phys. Rev. Lett.* **2003**, *91*, 146401.

(39) Krieger, J. B.; Chen, J.; Iafrate, G. J.; Savin, A. In *Electron Correlations and Materials Properties*; Gonis, A., Kioussis, N., Eds.; Plenum: New York, 1999.

(40) Zhao, Y.; Lynch, B. J.; Truhlar, D. G. *Phys. Chem. Chem. Phys.* **2005**, *7*, 43.

(41) Zhao, Y.; Truhlar, D. G. *J. Phys. Chem. A* **2004**, *108*, 6908.

(42) Zhao, Y.; Truhlar, D. G. *J. Phys. Chem. A* **2005**, *109*, 5656.

(43) Boese, A. D.; Handy, N. C. *J. Chem. Phys.* **2002**, *116*, 9559.

(44) Van Voorhis, T.; Scuseria, G. E. *J. Chem. Phys.* **1998**, *109*, 400.

(45) Dolg, M. In *Modern Methods and Algorithms of Quantum Chemistry*; Grotendorst, J., Ed.; John von Neumann Institute for Computing: Jülich, 2000; Vol. 1, pp 479−508.

(46) Martin, J. M. L.; Sundermann, A. *J. Chem. Phys.* **2001**, *114*, 3408.

(47) Chong, D. P. *Can. J. Chem.* **1995**, *73*, 79.

(48) Tsuchiya, T.; Abe, M.; Nakajima, T.; Hirao, K. *J. Chem. Phys.* **2001**, *115*, 4463; downloaded from: http://www.chem.t.u-tokyo.ac.jp/appchem/labs/ hirao/publications/dk3bs/bs046.html.

(49) Davidson, E. R. *Chem. Phys. Lett.* **1996**, *260*, 514.

(50) Martin, J. M. L.; De Oliveira, G. *J. Chem. Phys.* **1999**, *111*, 1843.

(51) Jensen, F. *J. Chem. Phys.* **2001**, *115*, 9113.

(52) See, for example, Iron, M. A.; Lucassen, A. C. B.; Cohen, H.; van der Boom, M. E.; Martin, J. M. L. *J. Am. Chem. Soc.* **2004**, *126*, 11699 and references therein.

(53) Dunning, T. H., Jr. *J. Chem. Phys.* **1989**, *90*, 1007.

(54) Woon, D. E.; Dunning, T. H., Jr. *J. Chem. Phys.* **1993**, *98*, 1358.

(55) Kendall, R. A.; Dunning, T. H., Jr.; Harrison, R. J. *J. Chem. Phys.* **1992**, *96*, 6796.

(56) A complete table of diffuse functions for the transition metals can be found in Supporting Information Table S2 of ref 52.

(57) Boys, S. F.; Bernardi, F. *Mol. Phys.* **1970**, *19*, 553.

(58) de Jong, G. T.; Geerke, D. P.; Diefenbach, A.; Sola, M.; Bickelhaupt, F. M. *J. Comput. Chem.* **2005**, *26*, 1006. (We thank a reviewer for bringing this paper and ref 59 to our attention.)

(59) de Jong, G. T.; Geerke, D. P.; Diefenbach, A.; Bickelhaupt, F. M. *Chem. Phys.* **2005**, *313*, 261.

(60) Boese, A. D.; Klopper, W.; Martin, J. M. L. *Mol. Phys.* **2005**, *103*, 863; *Int. J. Quantum Chem.* **2005**, *104*, 830.